Cell, Volume *130*

Supplemental Data

Self-Organization of MTOCs Replaces Centrosome Function during Acentrosomal Spindle Assembly in Live Mouse Oocytes

Melina Schuh and Jan Ellenberg

Supplemental Experimental Procedures

Image Processing and Quantitative Analysis

Microtubule nucleation rates at MTOCs were determined in 2D time series of microtubule plus ends labeled with EB3-mEGFP. For counting, the region surrounding the MTOC was divided into four quadrants. Nucleation events in every quadrant were counted three times, and the average values of all quadrants were summed up. As the measurements were performed in 2D time series, we underestimate the real nucleation rates approximately by a factor of ~3, taking into consideration that the optical slice thickness was about 2.1 µm, and that nucleation events could still be identified when the microtubule plus ends were in focus within a 1.5 µm radius around the MTOC.

To measure microtubule numbers (Figures 3C and 3D) in chromosomal proximity (distance from chromosomes ≤ 7 µm) and in the cytoplasm (distance from chromosomes > 7 µm), we recorded time-lapse sequences (single optical sections) of oocytes expressing H2B-mRFP1 to label chromosomes and EB3-mEGFP to label microtubule plus-ends, and analyzed the sequences with a macro implemented in ImageJ (http://rsb.info.nih.gov/ij/). The macro automatically detected chromatin regions in the H2B-mRFP1 channel by anisotropic diffusion filtering (Black et al., 1998) and thresholding, uniformly extended the chromatin region by 7

µm into all directions and computed the EB3-mEGFP fluorescence intensity inside of the identified region to obtain microtubule numbers in chromosomal proximity, and outside of the identified region to obtain microtubule numbers in the cytoplasm. For background correction, mean intensities outside of the oocyte were subtracted. To exclude signal from unbound EB3-mEGFP, the cytoplasmic intensity was measured in regions devoid of microtubule plus ends, and subtracted after background correction. For averaging of different experiments, we aligned the data to the time of NEBD determined by influx of soluble EB3-mEGFP, and normalized to the cytoplasmic intensity at NEBD. To determine the fraction of cytoplasmic nucleation, we calculated the ratio between microtubule nucleation in the cytoplasm and total oocyte nucleation given by the sum of chromosomal and cytoplasmic nucleation.

To quantify individual bivalent stretching (Figures 6A and 6D) we recorded 4D data sets (5 confocal sections, every 5 µm) of chromosomes labeled with H2B-mRFP1. We measured the angle between two bivalent arms over time. For averaging of different experiments, we interpolated the data to identical time intervals, aligned them to the time of biorientation (inter bivalent arm angle > 160°), and normalized to average initial and final angles.

To quantify total chromosome biorientation and spindle elongation (Figures 6B and 6E), we recorded 4D data sets (5 confocal sections, every 5 µm) of chromosomes labeled with H2B-mRFP1 and microtubules labeled with EGFP-MAP4 or microtubule plus ends labeled with EB3-mEGFP. We measured the spindle length over time and normalized to its initial and final length. For comparison of different experiments, we interpolated data to identical time intervals and aligned the different data sets to the time of half maximum spindle elongation. We determined the number of bioriented (inter bivalent arm angle > 160°) and unoriented (inter bivalent arm angle ≤ 160°) chromosomes for every time point and then computed the

fraction of bioriented chromosomes of all chromosomes given by the sum of bi- and unoriented chromosomes.

Supplemental Reference

Black, M. J., Sapiro, G., Marimont, D. H., and Heeger, D. (1998). Robust anisotropic diffusion. IEEE Transactions on Image Processing *7*, 421-432.

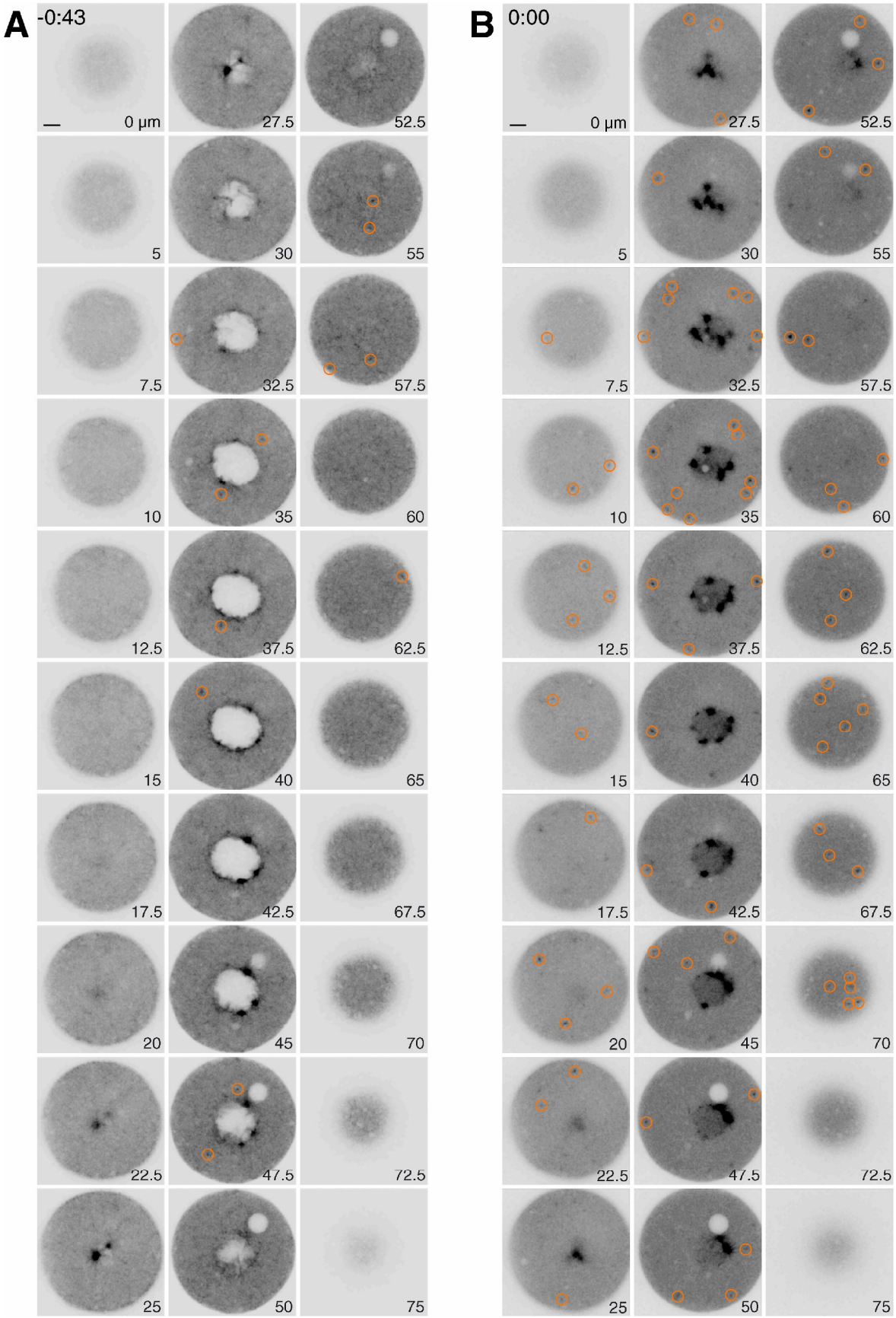
A
-0:43
0 µm
27.5
52.5
5
30
55
7.5
32.5
57.5
10
35
60
12.5
37.5
62.5
15
40
65
17.5
42.5
67.5
20
45
70
22.5
47.5
72.5
25
50
75
B
0:00
0 µm
27.5
52.5
5
30
55
7.5
32.5
57.5
10
35
60
12.5
37.5
62.5
15
40
65
17.5
42.5
67.5
20
45
70
22.5
47.5
72.5
25
50
75

Figure S1. Aster formation

Optical sections of a 4D data set similar to Figure 1B of a maturing oocyte expressing EGFP-MAP4 (microtubules) 43 minutes before NEBD (A) and at NEBD (B). MTOC positions are highlighted by yellow circles once in the optical section where they are best focused. The z-position of the different sections within the stack is indicated in µm. The white sphere in the cytoplasm is an oil droplet resulting from the microinjection procedure. Scale bar, 10 µm. Time, hh:mm relative to NEBD.

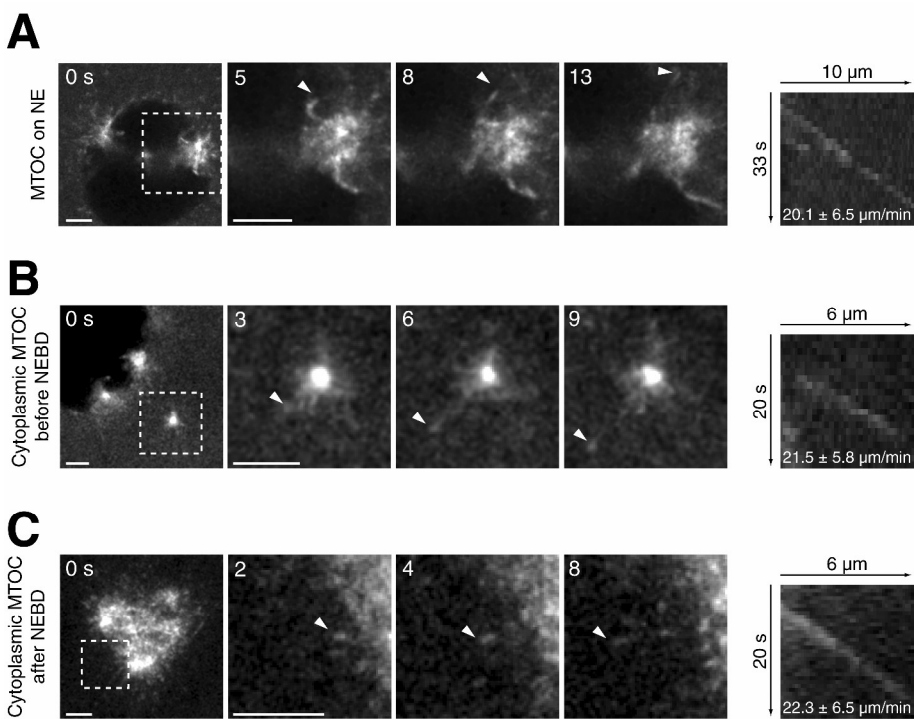

Figure S2. Velocities of MTOC nucleated microtubules

Determination of the growth rates of microtubules nucleated by MTOCs on the nuclear envelope (A), cytoplasmic MTOCs before (B) and after (C) NEBD in live mouse oocytes expressing EB3-mEGFP (left panels) via kymograph analysis (right panels). The boxed region in the overview image is magnified in the following images to visualize single microtubule plus ends. The kymograph corresponds to the microtubule plus end marked with white arrowheads. Kymograph analyses revealed that, before NEBD, microtubules nucleated at perinuclear MTOCs grew with a velocity of 20.1± 6.5 µm/min (A, n=15), not significantly different from microtubules nucleated at cytoplasmic MTOCs, which grew with a velocity of 21.5± 5.8 µm/min (B, n=21; p=0.49). After NEBD, the velocity of microtubule growth averaged 22.3± 6.5 µm/min (C, n=15), again not significantly different from microtubules nucleated before NEBD by either perinuclear or cytoplasmic MTOCs (p=0.36 and p=0.73). Scale bar, 5 µm. Time, seconds. See also Movie S4.

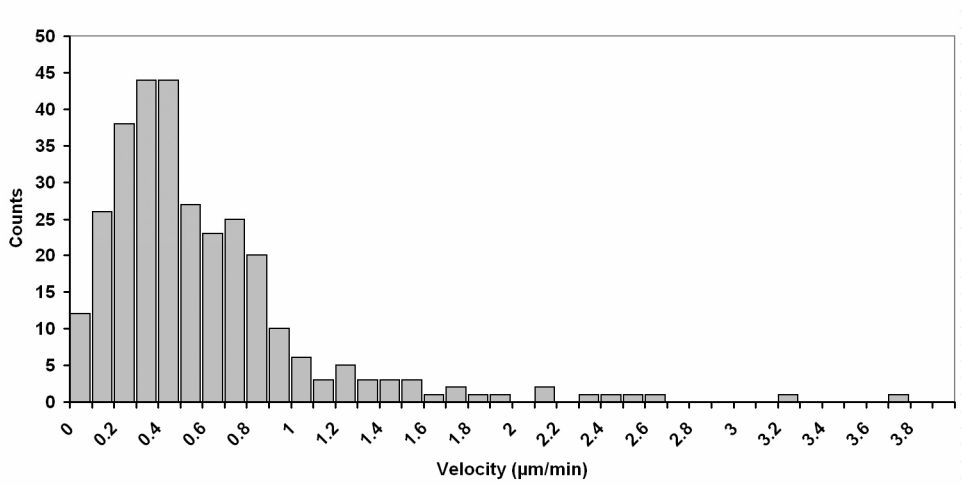

Figure S3. Histogram of MTOC velocities

Histogram was calculated from the data set presented in Figure 2C and five additional experiments. Total number of tracked MTOCs was 31.

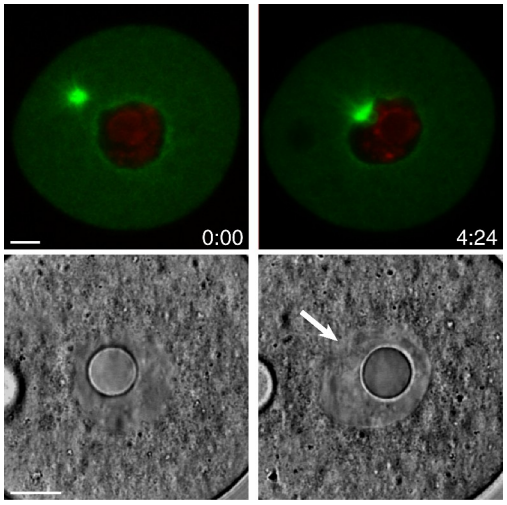

Figure S4. MTOCs move directly to the nuclear envelope and deform it

Time-lapse imaging of a maturing oocyte expressing EGFP-MAP4 (microtubules, green) and H2B-mRFP1 (chromosomes, red) (upper row) with maginified DIC of nuclear region (lower row). Arrow highlights MTOC induced invagination in the NE. Scale bar, 10 µm. Time, m:ss.

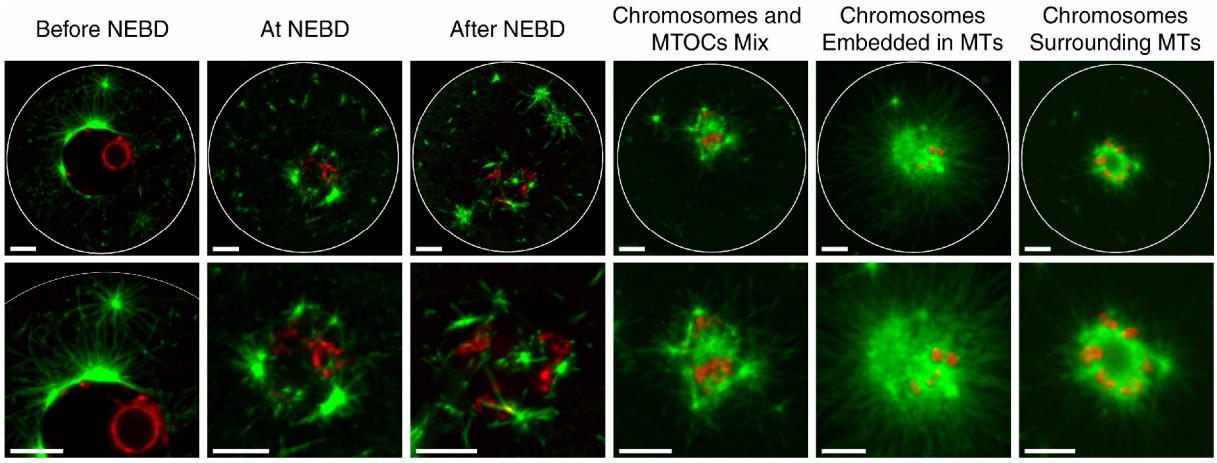

Figure S5. Microtubule nucleation during early spindle assembly

Immunofluorescence of oocytes fixed at different time points during meiotic maturation, as indicated above the top row. Bottom row shows magnified chromosome region. The white circle marks the oocyte rim. Microtubules are shown in green, chromosomes in red. Scale bar, 10 µm. See also Movie S5 for Chromosomes embedded in MTs.

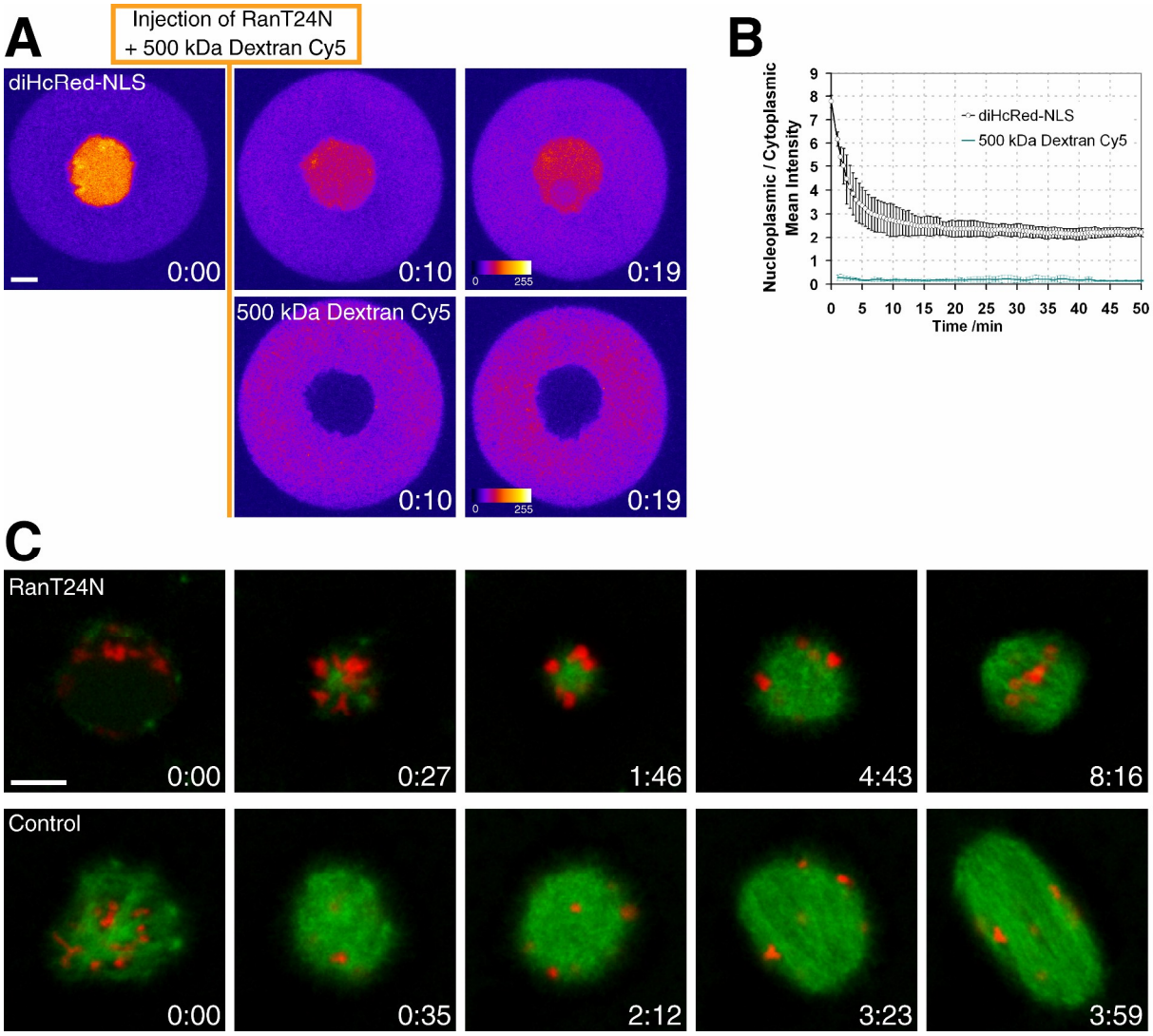

Figure S6. Test of RanT24N activity and delayed spindle assembly in RanT24N injected oocytes

(A) Time-lapse imaging of an oocyte that is arrested in prophase by dbcAMP and expresses the nuclear import marker diHcRed-NLS (pseudo-color representation, upper panel). After injection of RanT24N, diHcRed-NLS is released out of the nucleus into the cytoplasm. To confirm nuclear integrity after injection, a Cy5 labeled 500 kDa Dextran was co-injected (pseudo-color representation, lower panel). Look-up table is shown as a bar (last panels). Scale bar, 10 µm. Time, hh:mm.

(B) The ratio of nucleoplasmic to cytoplasmic mean intensity of diHcRed-NLS (black curve) or Cy5 labeled 500 kDa Dextran (green curve) is displayed. After reaching a steady-state distribution (~20 minutes after injection), the diHcRed-NLS intensity in the nucleus is approximately twice as bright as in the cytoplasm. This is partially due to the more crowded environment in the cytoplasm, but may also result from tetrameric diHcRed-NLS that

cannot diffuse out of the nucleus, and/or diHcRed-NLS that becomes sequestered within chromatin. Averages and standard deviations from three oocytes are shown. Time 0 refers to the time of injection.

(C) Time-lapse imaging of a maturing oocyte expressing EGFP-MAP4 (microtubules, green) and H2B-mRFP1 (chromosomes, red) after injection of RanT24N (upper panel) or in a control oocyte (lower panel). Scale bar, 10 μm. Time hh:mm.

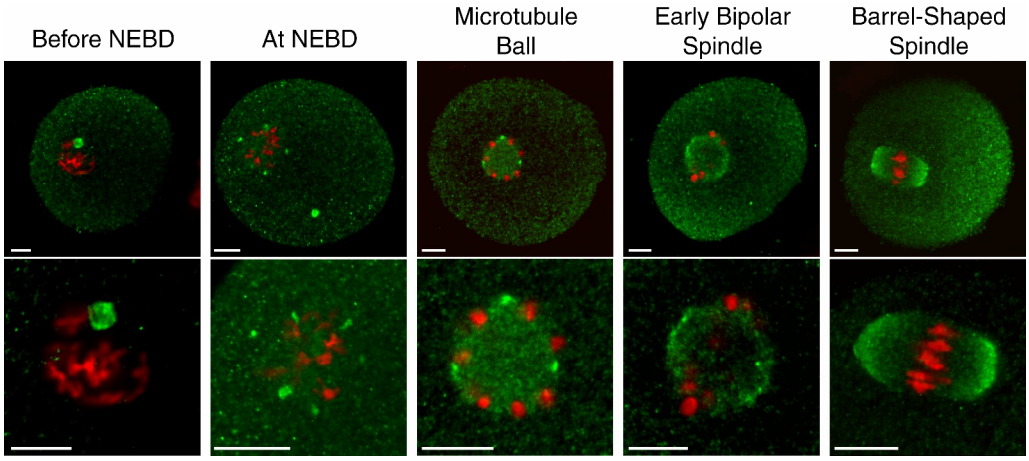

Figure S7. γ-tubulin localization during spindle assembly

Immunofluorescence staining of chromosomes (red) and γ-tubulin (green) in oocytes fixed at different time points after oocyte isolation (Before NEBD: 1 h, At NEBD: 1h, Microtubule Ball: 1h30min, Early Bipolar Spindle: 4 h, Barrel-Shaped Spindle: 8h after isolation). The spindle region is magnified in the bottom row. Scale bar, 10 μm.

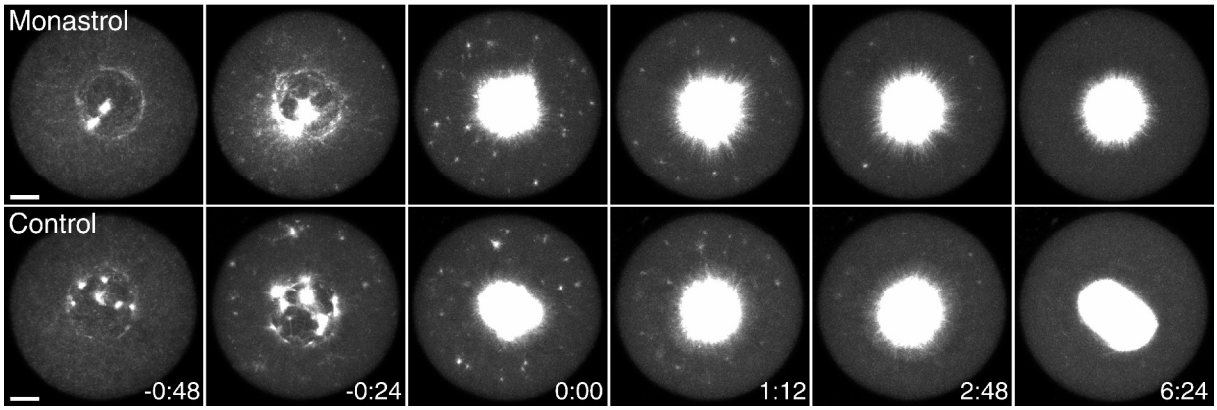

Figure S8. Kinesin-5 is not required for cytoplasmic MTOC recruitment

Z-projection (10 slices, every 5 µm) of maturing oocytes expressing EGFP-MAP4 (microtubules) that were treated with 100 µM monastrol (upper panel) or DMSO (lower panel). Scale bar, 10 µm. Time hh:mm.

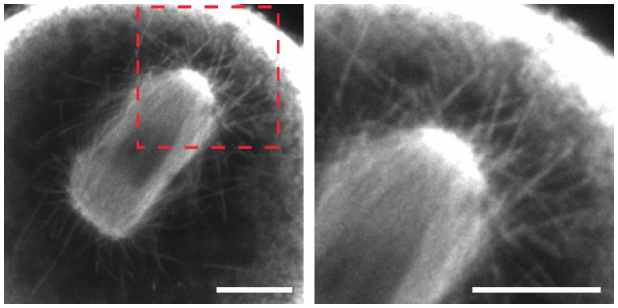

Figure S9. Acentrosomal spindle with astral-like microtubules

Immunofluorescence of tubulin showing the barrel-shaped spindle and astral-like microtubules in an oocyte fixed approximately 8 hours after NEBD. The boxed region is magnified in the right panel. Scale bar, 10 µm.

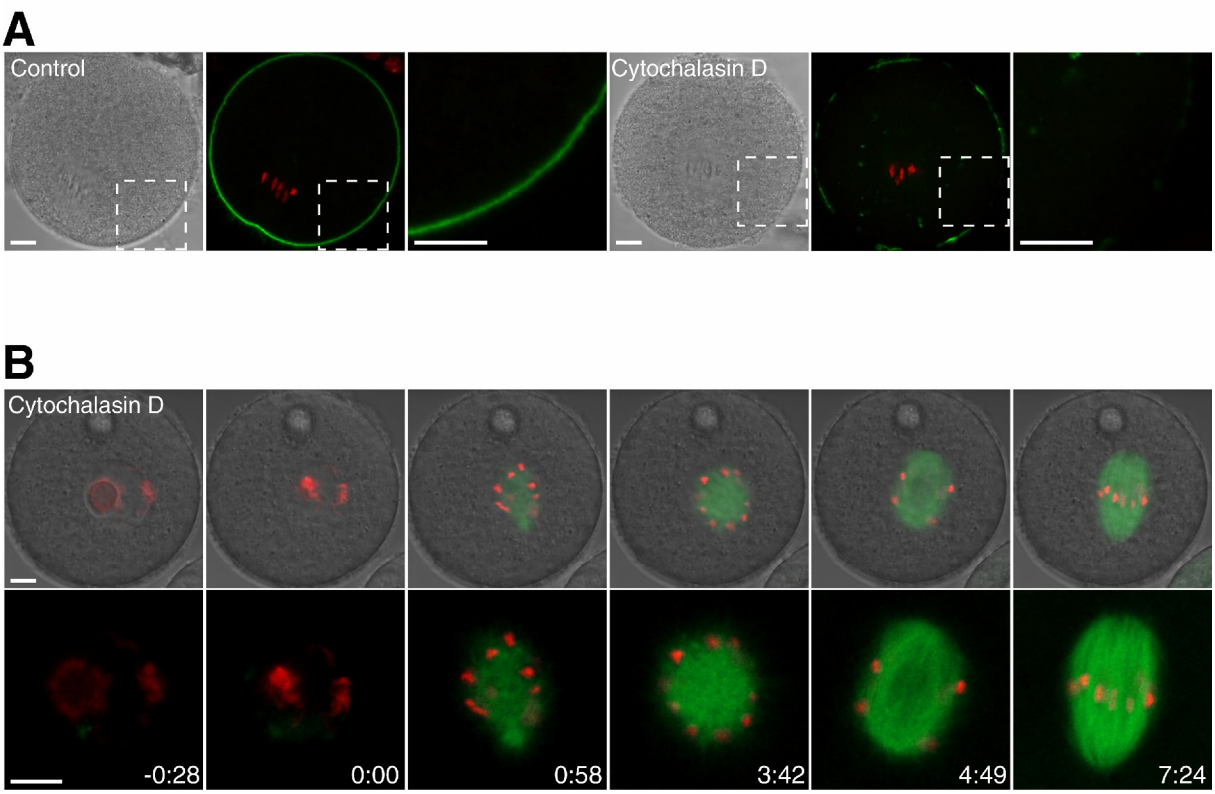

Figure S10. Spindle assembly does not require F-actin

(A) Immunofluorescence of oocytes treated with DMSO (left) or 3 µg/ml cytochalasin D (right). DIC, F-actin (green) and chromosomes (red) are shown. The boxed region in the overview images is magnified to visualize cortical staining in a region devoid of remnants of the zona pellucida. The green staining in the cytochalasin D treated oocyte corresponds to the position of remnants of the zona pellucida (see DIC). After depolymerization of F-actin by cytochalasin D, phalloidin unspecifically stain these zona pellucida remnants.

(B) A time-lapse series of oocyte maturation after depolymerization of F-actin by 3 µg/ml Cytochalasin D is shown. The oocyte expresses EGFP-MAP4 (microtubules, green) and H2B-mRFP1 (chromosomes, red). The sphere in the cytoplasm visible in the DIC channel is an oil droplet resulting from the microinjection procedure. Scale bar, 10 µm. Time, hh:mm relative to NEBD.